

AN INTEGRATED RF MEMS TUNABLE FILTER

Yonghyun Shim, Jia Ruan, Zhengzheng Wu, and Mina Rais-Zadeh

University of Michigan, Ann Arbor, MI 48109, USA

ABSTRACT

This paper reports on a high-performance MEMS lumped bandpass filter continuously tuned from 1 GHz to 0.6 GHz using 12 electrostatically actuated MEMS capacitors. To demonstrate the benefits of MEMS technologies, a reconfigurable filter array is implemented on a PCB using SMT components and its performance is compared to that of the MEMS filter. Besides the advantage in size, the MEMS filter also exhibits lower loss and greater rejection. To become a viable solution for RF applications, other performance specifications of MEMS filters such as tuning speed and reliability need to be improved.

INTRODUCTION

Reconfigurable UHF front-end filters can find numerous applications from multi-band TV tuners to mobile military radios. Filter requirements for such applications include wide frequency band coverage, low insertion loss, and high power handling capability, all in a small size and at low cost. Filter implementations using integration of passives with varactor diodes or employing MEMS capacitors on PCB can satisfy only a few of these requirements [1]-[3] (Table 1). Integration of separately packaged passives not only results in additional loss, but also derives increased fabrication cost and size. Size reduction using a multi-layer PCB technology is possible. However, reported filters using such technologies have failed to show a proper filter response across the tuned frequency spectrum mainly because of the low Q of passives embedded in the lower PCB layers.

In this paper, two technologies are considered for the implementation of lumped band-pass filter: fully integrated surface micromachining technology and PCB technology using surface mounted off-chip components. The integrated micromachined filter is continuously tuned using micro-electromechanical systems (MEMS) tunable capacitors with tuning ratio of more than 5:1 [4]. The frequency range of 600 MHz to 1 GHz is covered using a single MEMS tunable filter, reducing the required chip area. A different configuration is employed for the off-chip filter on PCB. The operating frequency range is covered by five non-overlapping third-order Butterworth filters connected to the input node using two gallium arsenide based RF switches. It is shown that the integrated MEMS filter has a smaller size and a better filter response, while the PCB filter has faster switching speed and higher power handling capability.

DESIGN

Target specifications of the lumped band-pass filter is shown in Table I. To cover a wide frequency range, two approaches can be taken. First, a number of filters can be placed in an array and connected to the input via a switch; a specific band can be selected by turning on the corresponding switch. Using this approach, no tunable passive component is

needed and each filter is fully matched to the termination impedance and optimized for the maximum performance. Therefore, the switching speed and power handling would be decided by the switch. An alternate approach would be to use tunable components to alter the frequency. The advantage of this approach is that the chip size can be significantly reduced. However, several tunable components are needed to not only tune the frequency but also ensure the filter is matched across the entire tuning range and the bandwidth requirement is met.

Table 1: Target specifications of filters

Specifications	Target values
Frequency coverage	600 MHz ~ 1000 MHz
Insertion loss @ center freq.	< 4 dB
3dB bandwidth (BW_{3dB})	12 ~ 15 %
Shape factor (BW_{30dB}/BW_{3dB})	< 4
Group delay	< 10 nsec
Tuning speed	< 50 μ sec
IIP_3	> 20 dBm

Integrated MEMS Filter

The first approach is based on a MEMS surface micromachining technology, which offers three metal, one dielectric, and two polymer sacrificial layers, allowing implementation of diverse passive components [5]. Using this technology, a third-order Chebyshev filter is implemented (Fig. 1 (a)). Mutual inductive coupling and inductive matching are used which exhibit wideband frequency matching and thus need not to be tuned when tuning the filter. To achieve wide frequency tuning, large-value and wide-tuning range capacitors are needed. To this end, a network of three capacitive switches and one continuously tuned capacitor (varactor) is incorporated in each resonator tank (Fig. 1 (b)). An equal final state value for varactors and capacitive switches ensures continuous tuning of the center frequency. The design procedure of the filter is discussed in detail in [6].

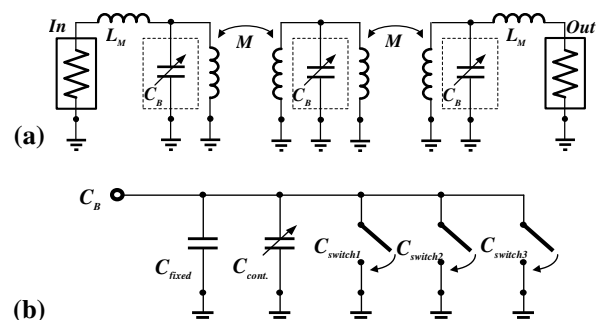


Figure 1: (a) Schematic view of a third-order bandpass filter, having three tunable capacitor banks. (b) Detail composition of each tunable capacitor bank.

To overcome the pull-in limitation and increase the tuning range, a dual-gap configuration is used for the varactors, with actuation to sense gap ratio of 4:1 [4]. All other capacitive switches in the bank are based on a similar

design, but the gap ratio is reduced to improve the linearity and ease of tuning. The 3D model of the filter used in simulations is shown in Fig. 2 (a), and the electromagnetic simulation result using ANSYS HFSS [7] is shown in Fig. 2 (b). As shown, all tuned states of the filter exhibit an insertion loss of less than 4 dB, bandwidth of 13~15%, out-of-band rejection of better than 40 dB, and group delay of less than 10 nsec (not shown).

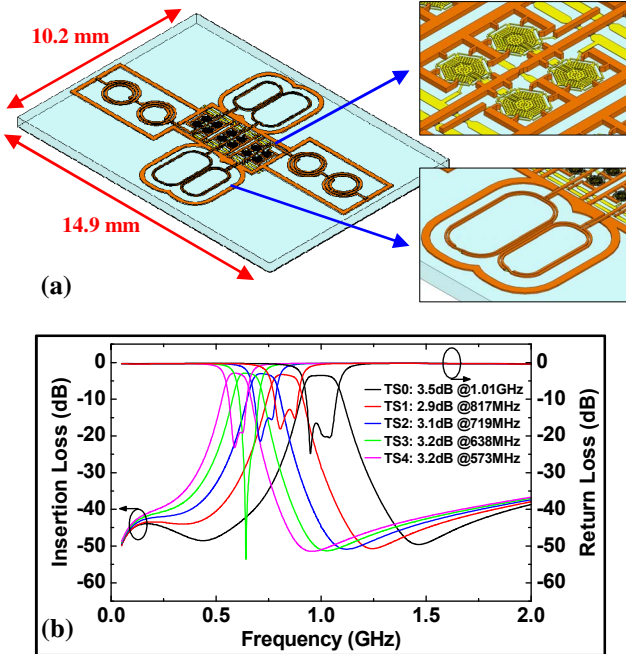


Figure 2: (a) A 3D model of the integrated MEMS filter. (b) HFSS simulation results of the filter at five tuned states.

Filter Array on PCB

The second approach is based on a switchable filter bank using discrete components on PCB. The filter array is shown in Fig. 3 (a). It is comprised of two single-input multiple-output switches connected to a bank of five fixed filters. This filter array can potentially achieve high linearity and good power handling capability due to the good linearity of the solid state switches at the frequency range of interest. In addition, as the matching and coupling are optimized for each filter, the filter array can provide the desired bandwidth and out-of-band rejection at each switched filter state.

Each filter within the filter array is designed as a third-order Butterworth band-pass filter in a capacitively coupled resonator configuration, as shown in Fig. 3 (b). The Butterworth filter configuration provides sharper cutoffs than linear phase filter and smaller pass-band ripples than Elliptic or Chebychev filter topology [8]. Capacitive coupling was employed instead of inductive coupling as the matching required here is for a narrow band and capacitors exhibit higher Q s than inductors, resulting in a lower filter loss. Values of L_1 and L_2 are fixed at 10 nH during the initial design process, and capacitor values are selected according to normalized design tables in [8], considering the target specifications.

To achieve fast switching, switches from Skyworks with switching time of sub-micro second are selected [9]. Selected switches are single-input four-output, thus two of

such switches are needed to control the five filters shown in Fig. 3 (a). Three DC voltage sources are needed for biasing; one is set to 5 V to turn on the switch, and the other two are set to either 0 V or 5 V to activate either one of the filters in the filter array. The size of the filter array could be reduced if only one switch was used instead of two. However, by using two switches, the length of the routing lines can be reduced and higher frequency filters can be placed closer to the input. To reduce high frequency parasitics, each filter is surrounded by a low-loss ground ring. The top ground ring is connected to the bottom ground using several through-chip vias, as shown in Fig. 4.

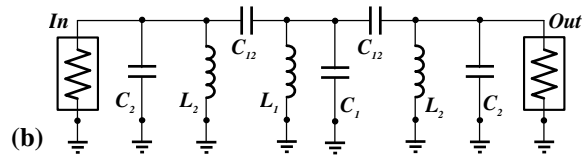
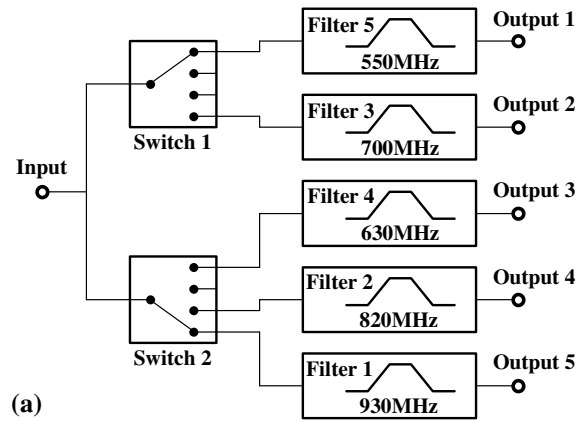


Figure 3: (a) A schematic of the PCB band-pass filter array, and (b) a schematic showing the configuration of each individual filter within the filter array.

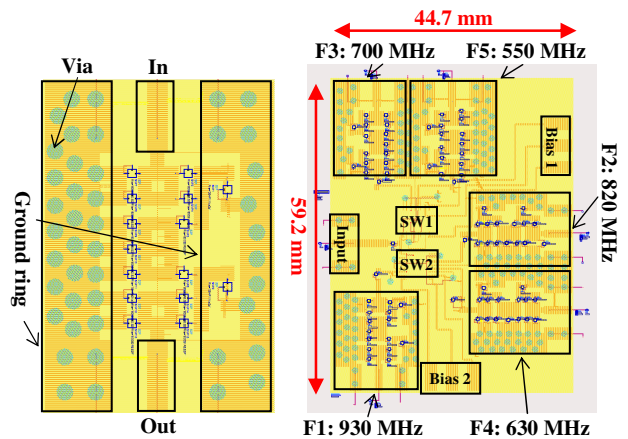


Figure 4: Layout of individual filters (left) and layout of the entire filter array (right).

Initial electrical design of the filters was simulated using Agilent ADS [10]. Full-wave electromagnetic simulations on the layout of the filter array are carried out using ADS momentum [10]. Simulated S-parameters of the filter array are shown in Fig. 5. All filters exhibit an insertion loss of less than 4 dB and out-of-band rejection of better than 40 dB. The group delay of all filters is less than

10 nsec (not shown).

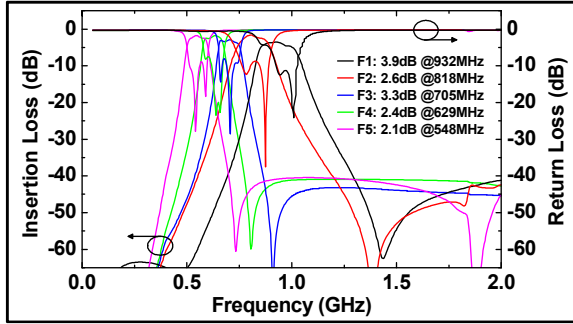


Figure 5: Simulated S -parameters of the filter array using ADS momentum analysis.

MEASURED RESULT & DISCUSSION

Figure 6 shows SEM views of the fabricated MEMS tunable filter. A photo graph of the entire MEMS filter together with an image of the PCB filter bank are shown in Fig. 7. The size of the MEMS filter is $10.2 \text{ mm} \times 14.9 \text{ mm}$, while that of the PCB filter array is $44.7 \text{ mm} \times 59.2 \text{ mm}$, using minimum feature size of $25 \mu\text{m}$. The size of the PCB filter array could be reduced using a PCB technology with a smaller minimum feature size. Nevertheless, the MEMS filter is much smaller than the PCB filter array for the same target frequency coverage.

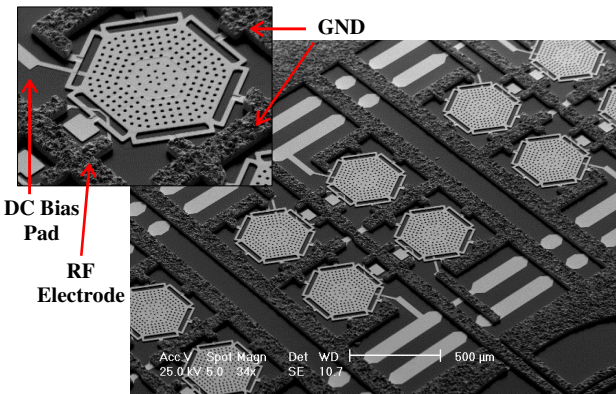


Figure 6: SEM images of the fabricated MEMS filter.

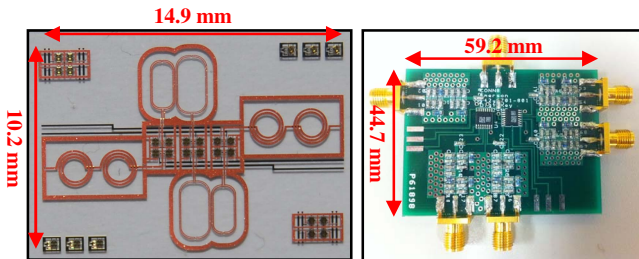


Figure 7: Photo graphs of a fabricated MEMS filter (left) and a filter array on PCB (right).

S -parameter measurements of filters are carried out using an Agilent N5241A network analyzer. PCB filters exhibit an insertion loss of 4.6 dB to 5.3 dB and an out-of-band rejection of 35 dB to 45 dB (Fig. 8). The discrepancies between measured and simulated performance of the PCB filter array is mainly due to the added loss of the solder connections. Figure 9 shows the measured insertion loss and return loss of the MEMS

tunable filter. The insertion loss at different tuned states ranges from 3.0 dB to 3.6 dB, while a constant percentage bandwidth of $\sim 13\%$ is maintained. The out-of-band rejection is more than 30 dB. The group delay is also measured to be less than 10 ns, as shown in Fig. 10.

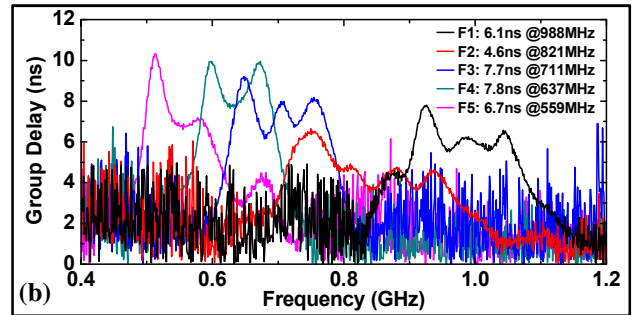
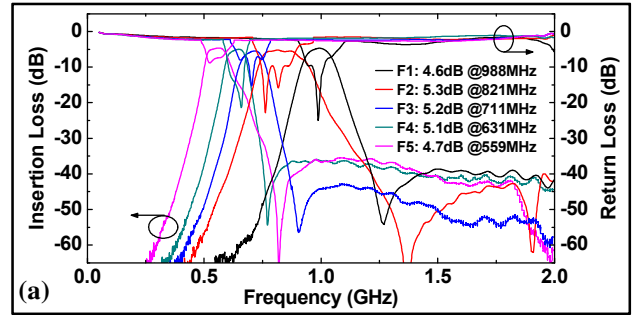


Figure 8: Measured (a) S -parameters and (b) group delay of the PCB band-pass filter array.

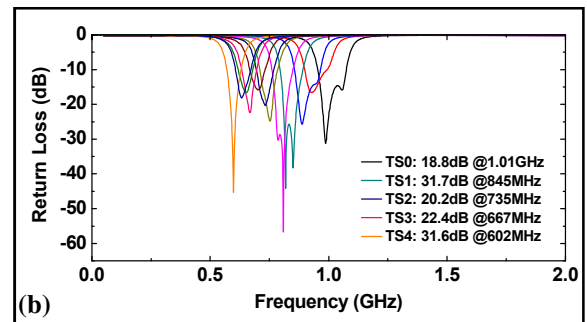
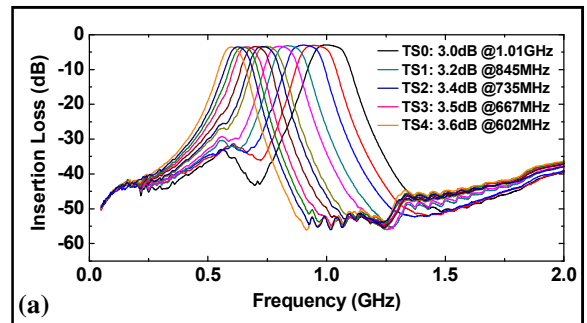


Figure 9: Measured (a) insertion loss and (b) return loss of the MEMS filter at various tuned states.

Figure 11 shows tuning speed of the MEMS filter and the switching speed of the PCB filter array, respectively. The tuning speed of the MEMS filter is between $40 \mu\text{s}$ to $80 \mu\text{s}$, depending on the applied tuning bias. The PCB filter array has a switching speed of less than $1 \mu\text{s}$. The output power spectrum of each filter is shown in Fig. 12.

The extracted IIP₃ of the MEMS filter at 100 kHz of frequency is ~27 dBm whereas that of the PCB filter array is more than 30 dBm. The IIP₃ of the MEMS filter depends on the tuning bias on the varactor and the frequency offset and ranges from 20 to 30 dBm [6].

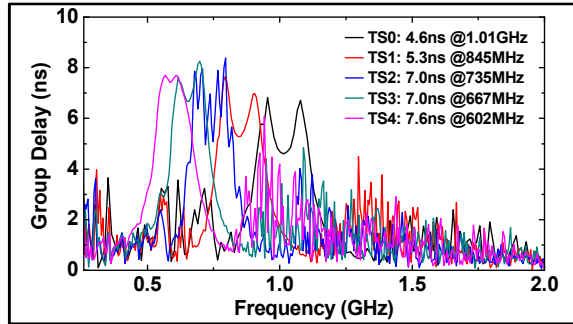


Figure 10: Measured group delay of the MEMS filter at each tuned state.

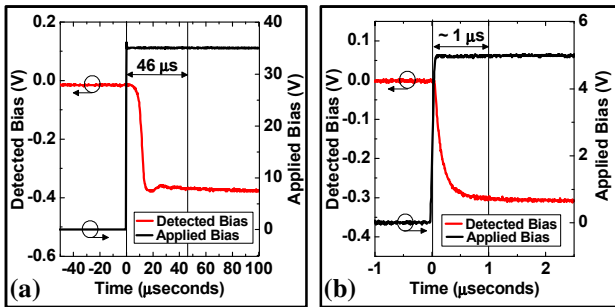


Figure 11: (a) Tuning speed of the MEMS filter; (b) switching speed of the PCB filter.

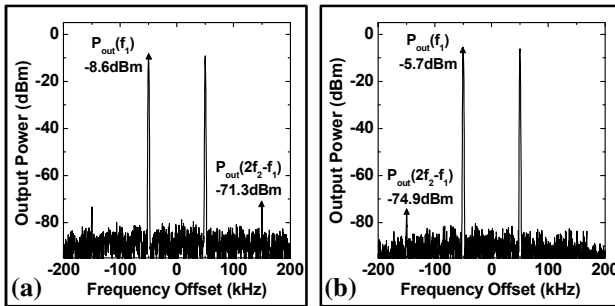


Figure 12: Output power spectrum; (a) the MEMS filter at -4 dBm input power; (b) the PCB filter at 0 dBm input power. Both measurements with 100 kHz frequency offset.

The measured specifications of the filters implemented using both technologies are summarized in Table I and compared to previous works. As expected, the PCB filter offers higher IIP₃ and faster tuning speed. However, the insertion loss and return loss of the MEMS

filter are better than the PCB filter due to the additional loss of interconnects and resistance of the solders used for connecting the off-chip elements on board. Compared to other works and the PCB filter array, the proposed MEMS filter shows the best published performance in a similar frequency range with a reasonably small foot-print.

CONCLUSIONS

MEMS and PCB technologies are compared for the implementation of UHF reconfigurable filters. The PCB filter is implemented using high-*Q* off-chip components with inductor *Q*s exceeding 100 [11] while the *Q* of the MEMS inductors is about 50. The MEMS filter with lower-*Q* passives has higher performance in terms of loss. To become a viable solution for multi-band radios, other performance specifications of the MEMS filters such as tuning speed and reliability need to be further improved.

ACKNOWLEDGEMENTS

This project was funded by Harris Corporation and by National Science Foundation (Award #1055308). Authors would like to thank staff members at the Michigan Nanofabrication Facilities (LNF) for their assistance.

REFERENCES

- [1] A. R. Brown, et al, "A varactor-tuned RF filter," *IEEE Transactions on Microwave Theory and Techniques*, Vol. 48, No. 7, July 2000.
- [2] R. L. Borwick, et al, "Variable MEMS capacitors implemented into RF filter systems," *IEEE Transactions on Microwave Theory and Techniques*, Vol. 51, No. 1, Jan. 2003.
- [3] T. C. Lee and J. Y. Park, "Compact PCB embedded tunable filter for UHF TV broadcasting," *IEEE IMS*, pp. 505-508, June 2009.
- [4] Y. Shim, et al, "A high-performance, temperature-stable, continuously tuned MEMS capacitor," *IEEE MEMS Conf.*, pp. 752-755, Jan. 2011.
- [5] Y. Shim, et al, "A multi-metal surface micromachining process for tunable RF MEMS passives," *Journal of Microelectromechanical System*, submitted.
- [6] Y. Shim, et al, "A high-performance continuously tunable MEMS bandpass filter at 1 GHz," *IEEE Trans. on Microwave Theory and Techniques*, submitted.
- [7] <http://www.ansoft.com/products/hf/hfss/>
- [8] Anatol I. Zverev, "Handbook of Filter Synthesis," *John Wiley and Sons*, 2005.
- [9] "AS204-80 data sheet," Skyworks Solutions, USA.
- [10] <http://www.agilent.com/find/eesof-ads/>
- [11] "0805CS data sheet," Coilcraft, IL, USA.

Table 1: Comparison between tunable front-end filters in UHF range

	Brown '00 [1]	Borwick '03 [2]	Lee '09 [3]	PCB filter array	This work
f_c	700-1330 MHz	225-400 MHz	510-910 MHz	559-988 MHz	602-1011 MHz
Insertion loss	2.0-6.0 dB	4.7-6.2 dB	1.8-2.5 dB	4.6-5.3 dB	3.0-3.6 dB
BW _{3dB}	8-22 % of f_c	4 % of f_c	20 % of f_c	8-15 % of f_c	13-14 % of f_c
BW _{30dB} /BW _{3dB}	2.0-3.0	5.0-6.0	4.5-6.5	2.8-3.6	3.2-4.7
Tuning Speed	N/A	< 600 μ s	N/A	< 1 μ s	40-80 μ s
IIP ₃	18-24 dBm	30-38 dBm	N/A	> 30 dBm	20-30 dBm
Technology	PCB (microstrip)	PCB + MEMS	PCB (multilayer)	PCB (SMT)	MEMS (single chip)
Size	31.0 \times 40.0 mm ²	30.0 \times 44.5 mm ²	4.4 \times 3.4 mm ²	44.7 \times 59.2 mm ²	10.2 \times 14.9 mm ²